

3D Convex Splatting: Radiance Field Rendering with 3D Smooth Convexes

Supplementary Material

6. Hyperparameters & Initialization

We initialize each convex shape using the COLMAP points as centers and uniformly distribute *new* points around them with the Fibonacci sphere algorithm to ensure an even distribution. The initial sphere radius is set to 1.2 times the mean distance to the three nearest neighbors in the point cloud. This adaptive initialization ensures that dense 3D regions contain many small convex shapes, while sparser regions are represented by larger convexes. The initial values for the smoothness parameter δ and sharpness parameter σ are set to 0.1 and $9.5e^{-4}$, respectively. These values are chosen to initially produce more diffuse shapes, as this configuration was empirically found to result in better performance during optimization. The initial opacity is set to 0.1. A detailed list of the hyperparameters can be found in Tab. 4.

7. Methodology Details

2D equations. We define the 2D convex indicator function for our convex hull by adapting the smooth convex representation from 3D to 2D, utilizing the equations introduced in Sec. 3.1. Specifically, we define $\phi(\mathbf{q})$ and $I(\mathbf{q})$ as in Eqs. (2) and (3), but substitute the 3D point \mathbf{p} with the 2D point \mathbf{q} and replace the planes delimiting the 3D convex hull with the lines that delimit the resulting 2D convex hull.

$$\phi(\mathbf{q}) = \log \left(\sum_{t=1}^T \exp(d \delta L_j(\mathbf{q})) \right), \quad (7)$$

where T is the total number of lines delimiting the 2D convex shape.

The indicator function $I(\mathbf{q})$ of the smooth convex is then defined by:

$$I(\mathbf{q}) = \text{Sigmoid}(-d \sigma \phi(\mathbf{q})). \quad (8)$$

8. Ablation Study

Perspective-Aware Scaling in 2D Projection. To incorporate perspective effects in the 2D projection, we scale δ and σ by the distance d , ensuring that the appearance of the convex shape remains consistent regardless of its distance from the camera. Table 5 provides an ablation study demonstrating the necessity of scaling δ and σ as well as analyzing the impact of the scaling magnitude.

9. More Results

Experiments on Synthetic Data. To highlight the effectiveness of our smooth convexes for rendering different shapes, we designed four 2D synthetic examples, where the optimization is performed in 2D, with a single image as ground truth. Figure 12 illustrates the optimization process of our smooth convexes on those four distinct shapes during training. Our convex shapes are highly versatile and capable of approximating a wide range of different shapes.

Real-world Novel View Synthesis. Figure 13 shows additional qualitative results, highlighting the capabilities of 3D Convex Splatting compared to 3D Gaussians and 2D Gaussians. The inherent softness of Gaussian primitives often leads to blurrier images and noticeable artifact-prone regions. While PSNR favors such blurrier images due to imprecise image alignment, they lack high-quality detail. Compared to Gaussian, 3D Convex Splatting does not produce any blurry areas and often results in a rendering much closer to the ground truth. For instance, in the *Bicycle* scene, Gaussian methods produce blurry artifacts on the street and in the grass, whereas 3D Convex Splatting achieves a result that closely matches the ground truth. Tables 6 to 11 show the complete quantitative results for each scene. 3D Convex Splatting outperforms 3DGS, 2DGS, and GES across all metrics on indoor scenes, the Deep Blending dataset, and the Tanks & Temples dataset.

Additional Visualizations. Figure 14 shows the depth maps obtained using 3D convexes vs. Gaussians, illustrating our better geometric quality, producing fewer artifacts and smoother depths. Furthermore, Fig. 15 shows the representation of a wall. It confirms that convexes generate denser and more physically accurate wall representations, whereas Gaussians produce more diffused shapes.

Table 4. Hyperparameters for Convex Splatting

Parameter	Indoor		Outdoor	
	Normal	Light	Normal	Light
Number of training iterations		30,000		
position_lr_delay_mult		0.01		
position_lr_max_steps		30,000		
feature_lr		0.0025		
opacity_lr		0.01		
lambda_dssim		0.2		
densification_interval		200		
densify_from_iter		500		
opacity_reset		0.2		
opacity_reset_interval		3000		
remove_size_threshold		0.3		
min_opacity		0.03		
lr_mask		0.01		
lr_delta		0.005		
nb_points		6		
convex_size		1.2		
set_opacity		0.1		
set_delta		0.1		
opacity_cloning		0.5		
delta_scaling_cloning		1		
shifting_cloning		1		
set_sigma	$9 e^{-4}$	$9.5 e^{-4}$	$1 e^{-3}$	$9.5 e^{-4}$
densify_grad_threshold	$6 e^{-6}$	$2.5 e^{-5}$	$1 e^{-6}$	$2.5 e^{-5}$
lr_sigma	$4.5 e^{-3}$	$4.5 e^{-3}$	$4 e^{-3}$	$4.5 e^{-3}$
reset_opacity_until	5000	5000	18000	5000
scaling_cloning	0.7	0.63	0.6	0.63
sigma_scaling_cloning	0.85	0.88	0.88	0.88
mask_threshold	$2 e^{-2}$	$1 e^{-2}$	$1 e^{-2}$	$1 e^{-2}$
lr_convex_points_init	$4 e^{-4}$	$5 e^{-4}$	$5 e^{-4}$	$5 e^{-4}$
lr_convex_points_final	$4 e^{-6}$	$5 e^{-6}$	$5 e^{-6}$	$5 e^{-6}$
densify_until_iter	9500	9000	9000	9000
storage	32-bit precision	16-bit precision	32-bit precision	16-bit precision

Magnitude	Truck	Train	DrJohnson	Playroom
1	19.47	19.14	29.17	28.82
\sqrt{d}	25.49	21.41	29.49	29.98
d	25.65	22.23	29.54	30.08
d^2	7.08	8.91	8.42	8.99

Table 5. **Perspective-Aware Scaling in 2D Projection.** We evaluate the PSNR under varying scaling magnitudes.

	Truck	Train	DrJohnson	Playroom
3DGS	0.148	0.218	0.244	0.241
2DGS	0.173	0.251	0.257	0.257
GES	0.162	0.232	0.249	0.252
3DCS	0.125	0.187	0.238	0.237

Table 6. LPIPS score for T&T and DB datasets.

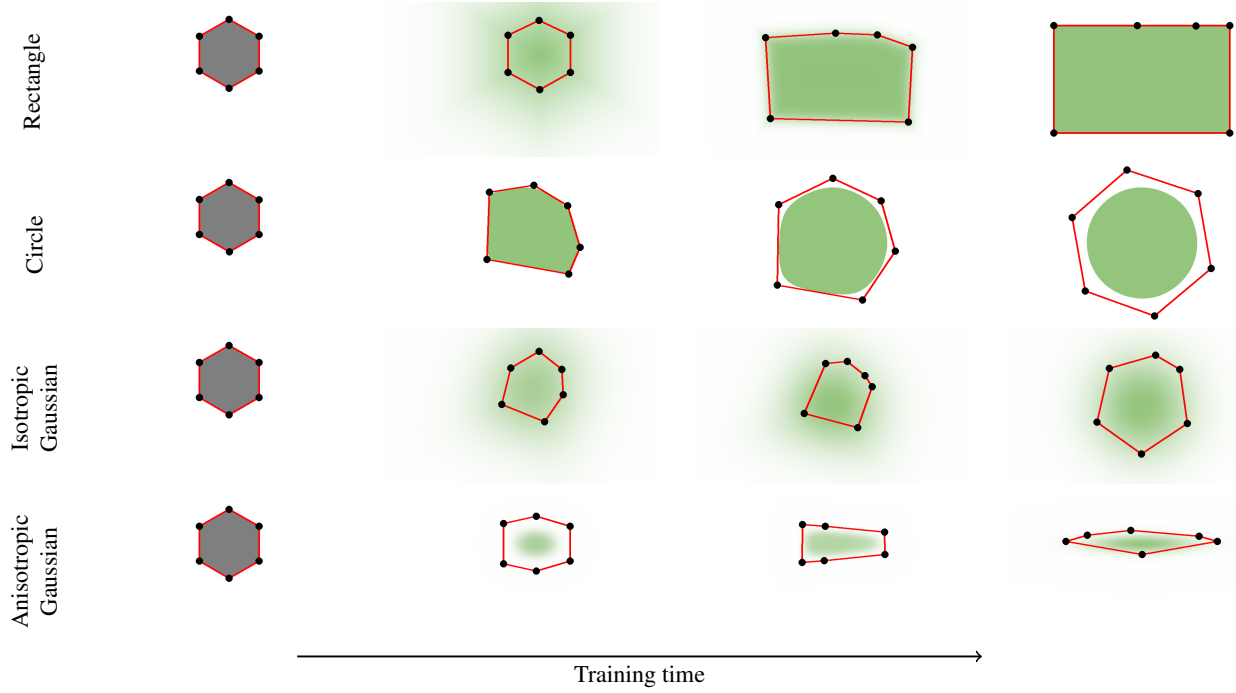


Figure 12. Smooth convexes can represent a wide variety of shapes, whether hard or soft, dense or diffuse. They effectively approximate diverse geometries, including both polyhedra and Gaussians, while requiring fewer primitives for accurate representation. The red lines describe the convex hull, whereas the black dots represent the point set.

	Truck	Train	DrJohnson	Playroom
3DGS	25.18	21.09	28.76	30.04
2DGS	25.12	21.14	28.95	30.05
GES	25.07	21.75	29.24	30.06
3DCS	25.65	22.23	29.54	30.08

Table 7. PSNR score for T&T and DB datasets.

	Bicycle	Flowers	Garden	Stump	Treehill	Room	Counter	Kitchen	Bonsai
3DGS	25.24	21.52	27.41	26.55	22.49	30.63	28.70	30.31	31.98
2DGS	24.87	21.15	26.95	26.47	22.27	31.06	28.55	30.50	31.52
GES	24.76	21.33	26.89	26.06	22.31	31.03	28.88	31.21	31.94
3DCS	24.72	20.52	27.09	26.12	21.77	31.70	29.02	31.96	32.64

Table 10. PSNR score for the MipNerf360 dataset.

	Truck	Train	DrJohnson	Playroom
3DGS	0.879	0.802	0.899	0.906
2DGS	0.874	0.789	0.900	0.906
GES	0.872	0.800	0.899	0.902
3DCS	0.882	0.820	0.902	0.902

Table 8. SSIM score for T&T and DB datasets.

	Bicycle	Flowers	Garden	Stump	Treehill	Room	Counter	Kitchen	Bonsai
3DGS	0.771	0.605	0.868	0.775	0.638	0.914	0.905	0.922	0.938
2DGS	0.752	0.588	0.852	0.765	0.627	0.912	0.900	0.919	0.933
GES	0.727	0.600	0.846	0.768	0.631	0.910	0.899	0.920	0.939
3DCS	0.737	0.575	0.850	0.746	0.595	0.925	0.909	0.930	0.945

Table 11. SSIM score for the MipNerf360 dataset.

	Bicycle	Flowers	Garden	Stump	Treehill	Room	Counter	Kitchen	Bonsai
3DGS	0.205	0.336	0.103	0.210	0.317	0.220	0.204	0.129	0.205
2DGS	0.218	0.346	0.115	0.222	0.329	0.223	0.208	0.133	0.214
GES	0.272	0.342	0.110	0.218	0.331	0.220	0.202	0.127	0.206
3DCS	0.216	0.322	0.113	0.227	0.317	0.193	0.182	0.117	0.182

Table 9. LPIPS score for the MipNerf360 dataset.

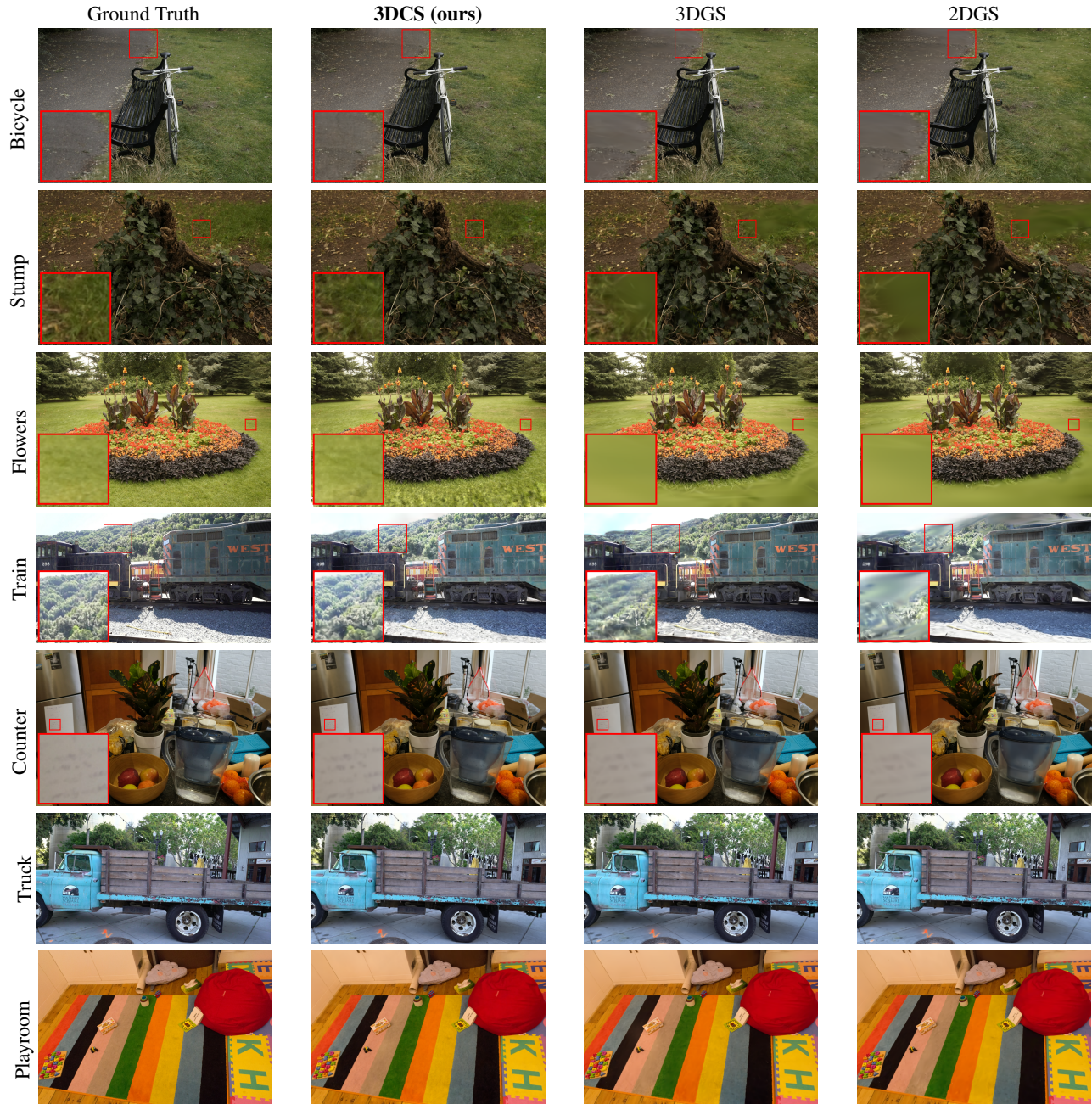


Figure 13. **Qualitative Comparison between 3DCS, 3DGS and 2DGS.** 3D Convex Splatting achieves high-quality novel view synthesis and fast rendering by representing scenes with 3D smooth convexes. In contrast, the softness of Gaussian primitives often results in blurring and loss of detail, while 3D Convex Splatting effectively captures sharp edges and fine details.

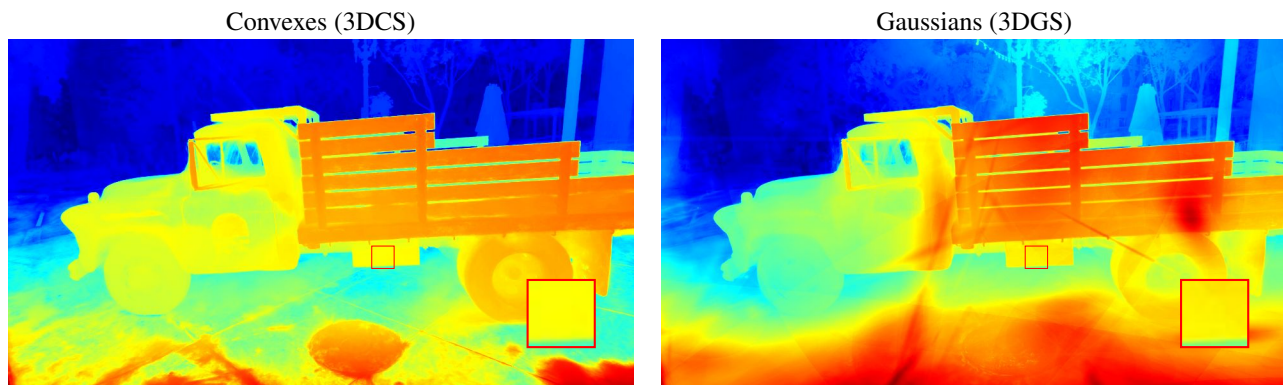


Figure 14. **Depthmap Comparison.** 3DCS generates fewer artifacts and a cleaner depth map than 3DGS.

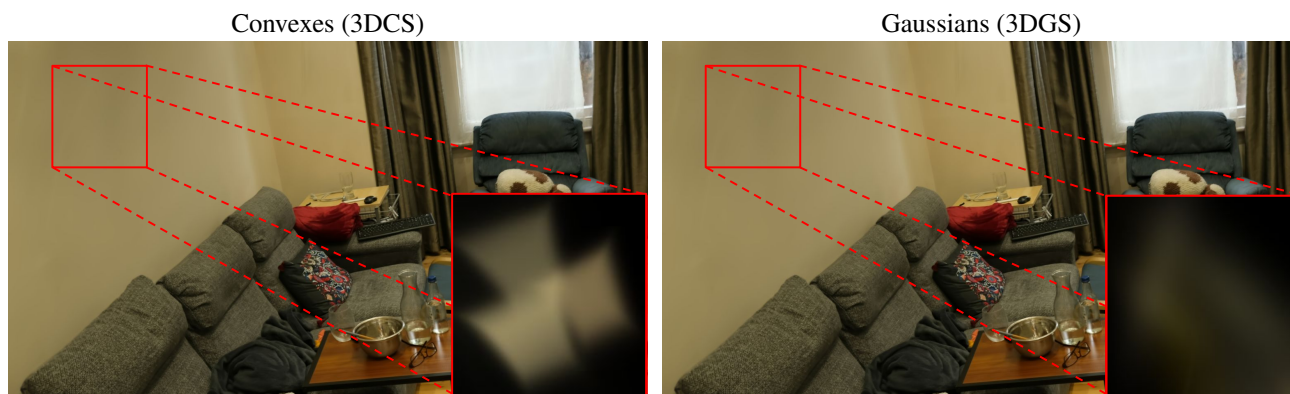


Figure 15. **Wall Approximation.** Example showing that 3DCS approximates a wall more uniformly and accurately than 3DGS.